IEEE Access
Multidisciplinary | Rapid Review | Open Access Journal

Received June 2, 2018, accepted July 9, 2018, date of publication July 13, 2018, date of current version August 7, 2018.

Digital Object Identifier 10.1109/ACCESS.2018.2855693

A Novel Fractal Contact-Electromechanical Impedance Model for Quantitative Monitoring of Bolted Joint Looseness

FURUI WANG[1], SIU CHUN MICHAEL HO[1], LINSHENG HUO[2], AND GANGBING SONG[1], (Member, IEEE)

[1]Department of Mechanical Engineering, University of Houston, Houston, TX 77204, USA
[2]School of Civil Engineering, Dalian University of Technology, Dalian 116024, China

Corresponding author: Gangbing Song (gsong@uh.edu)

This work was supported in part by the Major State Basic Research Development Program of China 973 Program under Grant 2015CB057704, in part by the general project of the Natural Science Foundation of China under Grant 51478080, and in part by the China Scholarship Council under Grant 201706060203.

ABSTRACT Bolted joint are among the key components that enable the robust assembly of a wide variety of structures. However, due to wear and tear over time, bolted joint may loosen, and if not detected in its early stages, can lead to devastating results. A monitoring method that can detect bolted joint looseness prior to bolt failure will be essential for the continued operation of the host structure and depending on the situation, the safety of the occupants. Prior research has proven the electromechanical impedance method (EMI) to be an effective technique for detecting the loosening of bolted joints, however, EMI-based methods until now are focused on qualitative health monitoring, which can only provide limited information about the damage. Thus, this paper attempts to quantify EMI based methods through the integration of fractal contact theory, the result of which is a novel electromechanical impedance model for quantitative monitoring of bolted looseness. The method determines the effective impedance of the bolted joint and is applied to develop the relationship between the electrical impedance of a piezoceramic patch installed on the joint and the mechanical impedance of the bolted joint. The mechanical impedance of the bolted joint under various preloads is computed by using the fractal contact theory. Then, the bolted looseness can be monitored quantitatively. At last, a set of verification tests under different applied preload of bolted joint are conducted to verify the validity of the proposed model in this paper.

INDEX TERMS Structural health monitoring, bolted looseness monitoring, electromechanical impedance modeling, fractal contact theory, piezoceramic transducers.

I. INTRODUCTION

As a fundamental structural connection, the bolted joint is used extensively in many engineering fields like railway, aerospace and petroleum, due to its low-cost and simplicity in fabrication [1]. However, a wide array of operational hazards such as cyclic loads, inappropriate manipulation, mechanical erosion, and chemical attack can initiate and accelerate damage of bolted joints [2], especially the relaxation of preload [3], and catastrophic consequences will occur if maintenance is not performed in a timely manner. With the widespread use of bolt connections in many key structures and a rising recognition of the potential dangers of bolt failure, the development of real-time monitoring method for bolted joint has become increasingly important. The conventional inspection techniques (e.g., visual and tapping inspection) can only provide limited, qualitative information, and more advanced methods, such as the ultrasound [4]–[6], the vibration-based methods [7]–[10], and the piezoelectric active sensing methods [11]–[14] often suffer from inferior sensitivity and may not always be able to detect early-stage bolted joint looseness.

Piezoceramic materials, which are highly flexible and multifunctional materials, have many uses including actuation [15], [16], sensing [17], [18], energy harvesting [19]–[21], communication [22], [23], and generation of guided waves [24], [25] for structural health monitoring purposes. One particularly attractive structural health monitoring technique based on the piezoceramic materials is the piezoelectric impedance-based method [26]–[33], which couples the electric impedance of the piezoelectric transducer and the host structure's mechanical impedance. In this technique, a Lead Zirconate Titanate (PZT) patch is bonded

on a structure and is driven by an alternating electric field. The alternating field causes the patch to strain at the same frequency and in turn generates stress waves that propagate along the structure. The stress waves can be used to obtain the structural vibration response, which is influenced by structural properties such as damping and stiffness. Conversely, strains of the structure can be transferred to the PZT patch, which will generate a measurable voltage. Thus, information about the structure can be determined by measuring and analyzing the electromechanical impedance (EMI) of the PZT patch. Compared with other structural health monitoring techniques, the piezoelectric impedance-based method has a notable advantage, i.e., a higher frequency range is used and thus it is sensitive to the small-scale damage. For such an advantage, the piezoelectric impedance-based method has been widely used for damage detection, such as in composite materials [34], aircraft components [35], gas pipelines [36], fatigue cracks [37], pin connections [38], truss structures [39], and concrete structures [40]. Recently, the piezoelectric impedance-based method has been extended to monitor bolt loosening [41]–[46]. However, all the above investigations only produce qualitative information, and is not based on any physical models potentially due to the difficulty and complexity in high-frequency structural modeling.

To study the EMI of coupled structures, analytical models characterizing electromechanical interaction between the PZT patch and the host structure need to be developed first. As of now, one-dimensional (1D) [47]–[49], two-dimensional (2D) [50]–[53] and three-dimensional (3D) [54], [55] models have been studied and reported. We should note that Bhalla and Soh [52], [53] also presented an improved 2D impedance model based on the concept of ''effective impedance'', which could predict the characteristics of the PZT-structure electromechanical interactions accurately. In addition, several analytical and semi-analytical models were developed to describe the dynamic interaction between the PZT transducers and the host structures, such as beams [56], [57], plates [58], cylindrical shells [59], [60] and so on. However, the literature about the EMI modeling of bolted joints is limited. Ritdumrongkul *et al.* [61], [62] developed the bonded-PZT beam model that describes both single and multiple bolted joint elements by using the spectral element method (SEM). In the model, the loosening of bolts could be quantitatively determined by measuring the electrical impedance of the PZT patch. However, the model is only valid for low frequency excitation. To the best knowledge of the authors, no published work has attempted EMI modeling of bolted joints at high frequencies.

The fractal contact theory [63], which is derived from the G-W contact model [64], is a powerful tool to study asperity interactions at structural interfaces and has been used in the study of bolted joint monitoring [65], [66]. Multiple investigations have been conducted to advance the fractal contact theory [67], [68], and through the foundation laid by studies on interfacial stiffness and damping [69], [70], and this paper will pave the way towards quantified EMI monitoring for bolted joints.

In this paper, based on the ''effective impedance'' modeling method proposed by Bhalla and Soh [52], [53], the relationship between the electric impedance of the PZT patch and mechanical impedance of the bolted joint at high frequencies is determined. An analytical model for computing the mechanical impedance of the bolted joint is developed by using the assumption that the bolted interface is equivalent to a mass-spring-damper mechanical system. The reason is that the deformation of asperities under bolted preload, which are the formation of interfacial roughness, can consume energy like damping. Additionally, considering the elastic recovery of asperities, we can also regard them as a spring in some ways. The interfacial stiffness and damping of bolted joint, both of which are affected by the preload, can be modeled based on the fractal contact theory. The fractal contact theory can then be used to obtain mechanical impedance of bolted joints. Finally, to verify the model, a set of experiments were conducted. The quantitative modeling of electro-mechanical of bolted joints presented in this paper can provide a good reference and guidance in particular application such as railway and aerospace engineering.

II. THEORETICAL BACKGROUND AND METHODOLOGY

A. ELECTROMECHANICAL IMPEDANCE MODELING OF BOLTED JOINT BASED ON THE CONCEPT OF EFFECTIVE IMPEDANCE

As shown in Figure 1, a PZT patch with finite sized square is bonded on the bolted joint surface, and it is subjected to a spatially harmonic electric field with an angular frequency ω. Considering the symmetry, i.e., the nodal lines coincide with the symmetry axes, thus consideration of 1/4 of the patch will suffice for studying the interaction of the patch and corresponding bolted joint. In (1), l is half the length of PZT patch, and f is the boundary traction per unit length, which respectively are related to planar deformations and area variations of the PZT patch. The study of the mechanical interaction between the PZT patch and the bolted joint extends over the entire PZT patch rather than just a point, unlike studies performed by other researchers. Therefore, several assumptions were proposed in this paper as in a prior study [52]: (1) the force from the PZT patch is transmitted along the entire boundary of the patch to the bolted joint, and the plane stress conditions exists within the patch; (2) the patch is regarded as an infinitesimal object to neglect its mass and stiffness; (3) the effect of the PZT vibrations in the thickness direction is ignored. Then, the ''effective mechanical impedance'' of the PZT patch is defined as [52],

$$Z_{a,eff} = \frac{\oint_s f \cdot \hat{n} ds}{\dot{u}_{eff}} = \frac{F}{\dot{u}_{eff}} \tag{1}$$

where F is the overall planar force, which leads to patch's area deformation; $\hat{n}$ is the unit vector normal to the boundary; $u_{eff} = \delta A / p_o$, which is defined as ''effective displacement'' of the patch; $\dot{u}_{eff}$ is the effective velocity, which is the

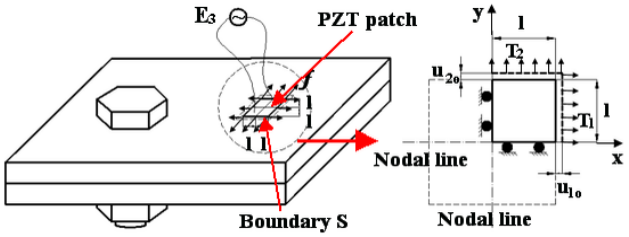

FIGURE 1. PZT patch bonded on the bolted joint and stresses/displacements on patch.

differentiation of effective displacement with respect to times; δA is the change of the patch surface area; p_o is the total lengths of patch's ''active boundaries''. It should be noted that $\oint_s f ds = 0$, to ensure equilibrium of overall force.

The constitutive relations for piezoelectric materials such as PZT are as follow [71],

$$\begin{bmatrix} D \\ S \end{bmatrix} = \begin{bmatrix} \overline{\varepsilon^T} & d^d \\ d^c & \overline{s^E} \end{bmatrix} \begin{bmatrix} E \\ T \end{bmatrix} \tag{2}$$

where $D(3 \times 1)$ is the electric displacement vector (C/m^2); $S(6 \times 1)$ is the strain vector; $E(3 \times 1)$ is the applied external electric field vector (V/m); $T(6 \times 1)$ is the stress vector (N/m^2); $\overline{\varepsilon_{ij}^T} = \varepsilon_{ij}^T(1 - \delta j)(3 \times 3)$ is the matrix of the complex dielectric permittivity at constant stress; $\overline{s_{km}^E} = s_{km}^E(1-\eta j)(6\times 6)$ is the matrix of the complex elastic compliance at constant electric field; $d_{im}^d(3 \times 6)$, $d_{jk}^c(6 \times 3)$ are the matrices of the piezoelectric strain coefficients; δ is the dielectric loss factor and η is the mechanical loss factor.

In this paper, the patch is assumed to be mechanically and piezoelectrically isotropic in the x-y plane, therefore, the PZT constitutive relations in (2) are reduced to

$$\begin{aligned} D_3 &= \overline{\varepsilon_{33}^T} E_3 + d_{31}(T_1 + T_2) \\ S_1 &= \frac{T_1 - \nu T_2}{\overline{Y^E}} + d_{31} E_3 \\ S_2 &= \frac{T_2 - \nu T_1}{\overline{Y^E}} + d_{31} E_3 \end{aligned} \tag{3}$$

where ν denotes the Poisson's ratio of the materials, $\overline{Y^E} = Y^E(1 + \eta j)$, is the complex Young's modulus of elasticity in a constant electric field. Then, (4) can be obtained algebraically,

$$T_1 + T_2 = \frac{(S_1 + S_2 - 2d_{31}E_3)\,\overline{Y^E}}{1 - \nu} \tag{4}$$

When the patch is in a zero-electric field (short-circuited), (4) can be rewritten as

$$(T_1 + T_2)_{short-circuited} = \frac{(S_1 + S_2)\,\overline{Y^E}}{1 - \nu} \tag{5}$$

Zhou *et al.* [72] proposed that the displacement of patch in the two principal directions were,

$$\begin{cases} u_1 = (A_1 \sin \kappa x) e^{j\omega t} \\ u_2 = (A_2 \sin \kappa y) e^{j\omega t} \end{cases} \tag{6}$$

where $\kappa = \omega\sqrt{\rho\left(1 - \nu^2\right)/\overline{Y^E}}$, is the wave number; A_1, A_2 are the coefficients which can be determined through boundary conditions; and ρ is the density of the PZT patch. The corresponding velocities and strains can be computed by differentiating (6) with respect to time and two coordinate axes,

$$\begin{cases} \dot{u}_1 = \dfrac{\partial u_1}{\partial t} = (A_1 j\omega \sin \kappa x) e^{j\omega t}; \\ \dot{u}_2 = \dfrac{\partial u_2}{\partial t} = (A_2 j\omega \sin \kappa y) e^{j\omega t} \\ S_1 = \dfrac{\partial u_1}{\partial x} = (A_1 \kappa \cos \kappa x) e^{j\omega t}; \\ S_2 = \dfrac{\partial u_2}{\partial y} = (A_2 \kappa \cos \kappa y) e^{j\omega t} \end{cases} \tag{7}$$

The effective displacement and the effective velocity of the PZT patch are given in terms of displacement u_{1o}, u_{2o} along x and y directions respectively, as shown in Figure 1.

$$\begin{cases} u_{eff} = \delta A / p_o = \dfrac{u_{1o} l + u_{2o} l + u_{1o} u_{2o}}{2l} \approx \dfrac{u_{1o} + u_{2o}}{2} \\ \dot{u}_{eff} = \dfrac{\dot{u}_{1o} + \dot{u}_{2o}}{2} = \dfrac{\dot{u}_{1(x=l)} + \dot{u}_{2(y=l)}}{2} \end{cases} \tag{8}$$

Then, the effective impedance of the patch can be obtained from (1), (5) and (7),

$$\begin{aligned} Z_{a,eff} &= \frac{\left(T_{1(x=l)} lh + T_{2(y=l)} lh\right)_{short-circuited}}{\left(\frac{\dot{u}_{1(x=l)} + \dot{u}_{2(y=l)}}{2}\right)} \\ &= \frac{2\kappa lh\overline{Y^E}}{j\omega(\tan \kappa l)(1 - \nu)} \end{aligned} \tag{9}$$

where h is the thickness of the PZT patch. The overall planar force F can be obtained as the expression of the mechanical impedance of the bolted joint $Z_{s,eff}$ [52],

$$\begin{aligned} F &= \oint_s f \cdot \hat{n} ds = T_{1(x=l)} lh + T_{2(y=l)} lh \\ &= -Z_{s,eff} \dot{u}_{eff} = -Z_{s,eff} \left(\frac{\dot{u}_{1(x=l)} + \dot{u}_{2(y=l)}}{2}\right) \end{aligned} \tag{10}$$

with $E_3 = (V_o/h)\, e^{j\omega t}$. By substituting (4) and (7), (11) can be obtained,

$$A_1 + A_2 = \frac{2d_{31} V_o Z_{a,eff}}{(\cos \kappa l) kh (Z_{s,eff} + Z_{a,eff})} \tag{11}$$

By integrating from $-l$ to $+l$ with respect to x and y, and substituting (3), (4), (7) and (11), we can obtain the admittance $\bar{Y}$, which is the reciprocal of the impedance.

$$\begin{aligned} \bar{Y} &= \frac{\bar{I}}{\bar{V}} = \frac{j\omega \iint_{A_1+A_2} D_3 dx dy}{\bar{V}} \\ &= 4\omega j \frac{l^2}{h} \left[\overline{\varepsilon_{33}^T} - \frac{2d_{31}^2 \overline{Y^E}}{(1-\nu)} + \frac{2d_{31}^2 \overline{Y^E} Z_{a,eff}}{(1-\nu)(Z_{s,eff} + Z_{a,eff})} \left(\frac{\tan \kappa l}{\kappa l}\right)\right] \end{aligned} \tag{12}$$

where $\bar{I}$ is the instantaneous electric current; $\bar{V} = V_o e^{j\omega t}$, is the instantaneous voltage through the patch. In other words, the electro-mechanical impedance of the bolted joints can be

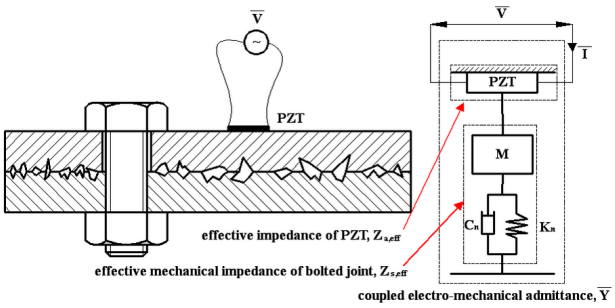

FIGURE 2. Micro contact of bolted joint surface with bonded PZT and its equivalent dynamic model.

computed by using (12), if the mechanical impedance of the bolted joint $Z_{s,eff}$ is known. The analytical modeling of $Z_{s,eff}$ will be given in the next Section.

B. MECHANICAL IMPEDANCE MODELING OF BOLTED JOINT USING THE FRACTAL CONTACT THEORY

The bolted interface is rough on the microscopic scale and thus is equivalent to a mass-spring-damper mechanical system due to the existence of the interfacial stiffness and damping, as illustrated in Figure 2. Based on the previous research results [73], the mechanical impedance $Z_{s,eff}$ of such a mass-spring-damper mechanical system can be expressed as,

$$\begin{cases} Z_{s,eff}\ real\ part = \dfrac{Cm^2\omega^2}{C^2+(\omega m - K/\omega)^2} \\ Z_{s,eff}\ imaginary\ part = \dfrac{m\omega\left[C^2 - \frac{K}{\omega}(\omega m - K/\omega)\right]}{C^2+(\omega m - K/\omega)^2} \end{cases} \tag{13}$$

where m is the mass of the mechanical system; C is the damping coefficient of the mechanical system; K is the stiffness of the mechanical system; and ω is the frequency. The interfacial damping and stiffness of bolted joint can be modeled by using the fractal contact theory to take the imperfect interface into account [63], and then the mechanical impedance of the bolted joint $Z_{s,eff}$ can be obtained.

Based on the Hertz contact theory [74], the relationship between the contact load and the normal deformation δ of the asperity can be described by [75],

$$\begin{cases} elastic\ deformation\ stage: P_e = \frac{4}{3}E^*R^{1/2}\delta^{3/2}; & \delta \le \delta_c \\ plastic\ deformation\ stage: P_p = 2H\pi R\delta; & \delta \ge \delta_c \end{cases} \tag{14}$$

where, P_e is the normal contact load in asperity's elastic deformation stage; P_p is the contact load in plastic deformation stage; R is the radius of asperity on rough surface; $\delta_c = \left(\frac{\pi H}{2E^*}\right)^2 R$, which is critical deformation of asperity determined by the Hertz contact theory; $E^* = \left[\left(1-\upsilon_1^2\right)/E_1 + \left(1-\upsilon_2^2\right)/E_2\right]^{-1}$, is the equivalent elasticity modulus; E_1 and E_2 are elasticity modulus of two contact materials, respectively; ν_1 and ν_2 are the Poisson's ratio of two contact materials respectively; $H = 2.8\sigma_s$ [76] is the hardness of the material; and σ_s is the yield strength of the material.

Considering the W-M fractal function [77], Wang and Komvopoulos [67] proposed a computational method for obtaining δ and R.

$$\delta = G^{D-1}a^{\frac{2-D}{2}};\ R = \frac{a^{D/2}}{2\pi G^{D-1}} \tag{15}$$

With knowledge of the two parameters, the critical truncated area of asperity a_c can be computed by $a_c = G^2\left(\frac{2E^*}{H}\right)^{2/(D-1)}$ when $\delta = \delta_c$, where a is the truncated area of asperity; D is the fractal dimension, G is the scaling constant, all of which can be calculated by the power spectrum of the W-M function, which describe the surface profile of the interface [77], [78]. Subsequently, the relationship between the contact load and the truncated area of asperity a can be described by,

$$\begin{cases} elastic\ deformation\ stage: P_e = \dfrac{4}{3\sqrt{2\pi}}E^*G^{D-1}a^{\frac{3-D}{2}}; \\ \qquad\qquad\qquad\qquad a \ge a_c \\ plastic\ deformation\ stage: P_p = Ha; \quad a \le a_c \end{cases} \tag{16}$$

The domain extension factor ψ was introduced to describe the size distribution function, and it can be computed by [16],

$$n(a) = \frac{D}{2}\psi^{(2-D)/2}a^{D/2}a^{-(D+2)/2} \quad 0 < a \le a_l \tag{17}$$

where a_l is the truncated area of the largest asperity. Then, the relationship between the normal contact load P^* and the actual contact area A_r of the entire bolted joint surface can be computed by the normalization method,

$$\begin{cases} P^* = \dfrac{P}{E^*A_a} = \dfrac{\int_0^{a_c} n(a)P_p(a)da + \int_{a_c}^{a_l} n(a)P_e(a)da}{E^*A_a} \\ = \dfrac{1}{3\sqrt{\pi}}G^{*(D-1)}g_1(D)\psi^{\frac{2-D}{2}}A_r^{*\frac{D}{2}} \\ \quad \left[\psi^{\frac{-D^2+7D-6}{4}}\left(\dfrac{2-D}{D}\right)^{\frac{3-2D}{2}}A_r^{*\frac{3-2D}{2}} - a_c^{*\frac{3-2D}{2}}\right] \\ \quad +2.8\varphi g_2(D)\psi^{(\frac{2-D}{2})^2}A_r^{*\frac{D}{2}}a_c^{*\frac{2-D}{2}} \quad (D \ne 1.5) \\ P^* = \dfrac{2^{\frac{1}{4}}}{\sqrt{\pi}}G^{*\frac{1}{2}}\psi^{\frac{1}{16}}\left(\dfrac{A_r^*}{3}\right)^{\frac{3}{4}}\ln\left(\dfrac{A_r^*}{3\psi^{\frac{1}{4}}a_c^*}\right) \\ \quad +8.4\varphi\psi^{\frac{1}{16}}\left(\dfrac{A_r^*}{3}\right)^{\frac{3}{4}}a_c^{*\frac{1}{4}} \quad (D = 1.5) \end{cases} \tag{18}$$

where, A_a is the nominal contact area; $G^* = \frac{G}{\sqrt{A_a}}$; $A_r^* = \frac{A_r}{A_a}$; $a_c^* = \frac{a_c}{A_a}$; $\varphi = \frac{\sigma_s}{E^*}$; $g_1(D) = 2^{\frac{6-D}{2}}\left(\frac{2-D}{D}\right)^{\frac{D}{2}}\frac{D}{3-2D}$; $g_2(D) = \left(\frac{D}{2-D}\right)^{\frac{2-D}{2}}$.

The relationship between the interfacial stiffness K_n and the actual contact area A_r of the entire bolted joint surface

can be computed by the normalization method,

$$\begin{cases} k_n = \dfrac{dP_e}{d\delta} = 2E^* R^{\frac{1}{2}} \delta^{\frac{1}{2}} = 2E^* \sqrt{\dfrac{a}{2\pi}} \quad \delta \le \delta_c,\ a \ge a_c \\ K_n^* = \dfrac{K_n}{E^* \sqrt{A_a}} = \dfrac{\int_{a_c}^{a_l} n(a) k_n da}{E^* \sqrt{A_a}} \\ \quad = \dfrac{2}{\sqrt{\pi}} g_3(D) \psi^{\left(\frac{2-D}{2}\right)^2} A_r^{*\frac{D}{2}} \\ \quad \left[\left(\dfrac{2-D}{D} \right)^{\frac{1-D}{2}} \psi^{\frac{-D^2+3D-2}{4}} A_r^{*\ \frac{1-D}{2}} - a_c^{*\frac{1-D}{2}} \right] \end{cases} \tag{19}$$

where $g_3(D) = \frac{D^{\frac{2-D}{2}}(2-D)^{\frac{D}{2}}}{1-D}$.

The damping loss factor η_C can be defined as the ratio of the plastic strain energy W_p to the elastic strain energy W_e of the interface, and therefore, can be expressed as follows,

$$\begin{aligned} \eta_C &= \frac{W_p}{W_e} = \frac{\int_0^{a_c} \int_0^{\delta} P_p n(a) d\delta da}{\int_{a_c}^{a_l} \int_0^{\delta} P_e n(a) d\delta da} \\ &= \frac{15\sqrt{2\pi} H (5-3D) a_c^{2-D}}{16 E^* G^{D-1} (2-D) \left(a_l^{\frac{5-3D}{2}} - a_l^{\frac{D}{2}} a_c^{\frac{5-3D}{2}} \right)} \end{aligned} \tag{20}$$

Assuming that the mass of the system is M, the relationship between the interfacial damping coefficient C_n and the actual contact area A_r of the entire bolted joint surface can be computed by the normalization method (21) , as shown at the bottom of the next page.

Based on the (18), (19) and (21), the effects of the normal contact load P of the bolted joint on the interfacial stiffness and the damping coefficient K_n, C_n can be obtained by using the actual contact area A_r as an intermediary, and then the mechanical impedance of the bolted joint can be determined when the applied preload is known. Interacting this relationship with the effective electro-mechanical modeling proposed in former Section, the quantitative monitoring of the bolted looseness based on the piezoelectric impedance method can be achieved.

III. EXPERIMENTAL SETUP

In this paper, the experimental setup for the proposed piezoelectric mechanical modeling method consisted of a PZT patch, an impedance analyzer, a computer with DAQ software system (NI), a torque wrench and a bolted joint. The specimen is placed on a bench vice. The PZT patch (size: 10mm×10mm×1mm) was mounted on the bolted joint surface by using epoxy resin, which was a joint composed of two rectangular steel plates (size: 150mm×80mm×20mm) fastened by a pair of M20 bolt and nut, as shown in Figure 3. Basically, the PZT patch with 1mm thickness is preferred for stronger actuation rather than sensing compromised sensory ability. However, considering the principle of piezoelectric impedance method is actuating structures based on piezoelectric material, we select the PZT patch with this thickness.

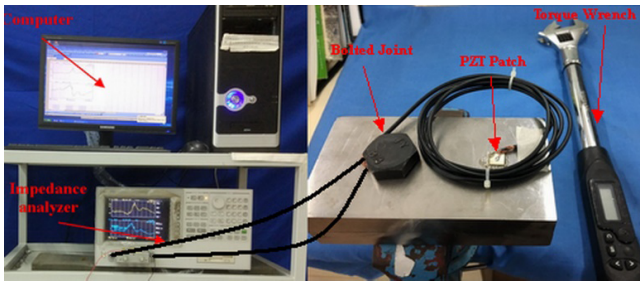

FIGURE 3. Photos of experimental setup.

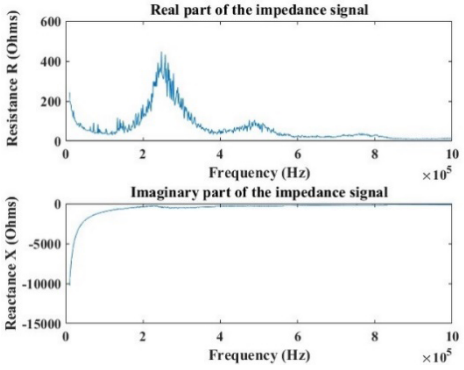

FIGURE 4. The results of sweep frequency under 70 N m (10 Hz - 1MHz).

The PZT patch was connected to a precision impedance analyzer (Agilent HP4294A), to measure the variations in the electrical impedance of the PZT patch bonded on the bolted joint surface under different preloads. A torque wrench was used to apply four torque level from 10 N m to 70 N m with increments of 20 N m.

Monitoring the change of electromechanical impedance of bonded PZT patch reveals the different mechanical properties of bolted joint under various preload like frequency shift and peak amplitude, which can be compared to the analytical results obtained in Section II. A computer equipped with DAQ software (National Instruments) is utilized to control the impedance analyzer, to extract impedance signals as a function of excitation frequency. Additionally, the selection of a suitable frequency range is important for the excitation signal, as the frequency range determines the detection sensitivity of the impedance-based method [79]. Therefore, a sweep frequency test with a range of 10 Hz - 1 MHz with 801 sampling data points was conducted to obtain the optimal frequency range (Figure 4) under 70 N m torque. It could be found that the real part of the electrical impedance signature was more sensitive to the variation in the bolted joint's mechanical properties (i.e., change in stiffness and damping due to axial preload). In contrast, the imaginary component was not nearly as sensitive, which is consistent with previous study result [80]. This difference in sensitivity can be attributed to the fact that the imaginary part of the electrical impedance is determined by the capacitive response of the PZT patch, which is less sensitive to the variation in the mechanical properties of bolted joints.

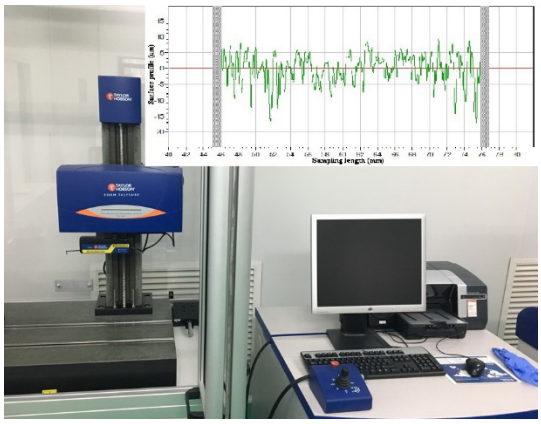

FIGURE 5. Talor Hobson surface profiler.

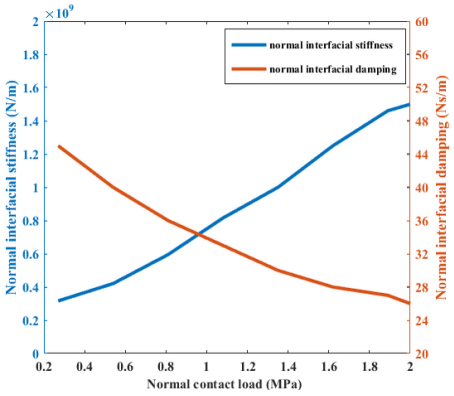

FIGURE 6. General trend of interfacial stiffness and damping.

Based on the frequency response in Figure 4, the frequency range from 100 kHz to 400 kHz was selected as the optimal frequency range for generation of excitation signals.

The material properties of the PZT patch and steel are given in Table 1. To compute the interface stiffness and damping coefficient described in Section II, the fractal parameters D and G were obtained by a phase grating interference surface roughness profiler (TALOR HOBSON, PGI 840, UK) depicted in Figure 5. As shown in Figure, the x-axis is sampling length, and y-axis is surface profile size. The detailed calculation method was given in [65], and the D and G measured by the profiler were 1.21 and 5.26×E-14, respectively.

TABLE 1. Material properties.

Material	Properties	Values	Unit
Steel	Young modulus	209	GPa
	Poisson ratio	0.3	
	Density	7860	kg m-3
	Brinell hardness	1.96	GPa
PZT	Density	7450	kg m-3
	Young modulus	46	GPa
	Poisson ratio	0.3	
	Piezoelectric coefficients $d_{31}, d_{32} / d_{33}$	0.186/0.42	nC N^{-1}
	Dielectric coefficients $\varepsilon_{11}, \varepsilon_{22} / \varepsilon_{33}$	0.15/0.13	nF N^{-1}
	Dielectric loss factor	0.02	
	Mechanical loss factor	0.001	

IV. RESULTS AND DISCUSSION

Based on the fractal parameters D and G obtained from the surface profile measurement, and the interfacial stiffness and the damping modeling obtained from the fractal contact theory proposed in Section II, the relationship between the interfacial stiffness/damping and the normal preload of the bolted joint interface can be estimated, as shown in Figure 6. The normal contact pressure in this paper is defined as the ratio between the axial preload and the nominal contact area of the bolted joint interface. It can be observed that the interfacial stiffness increases with the increase of applied torque. The decreasing slope as the load was increased suggests an approach towards saturation, which is consistent with the previous research results [81]. The variation in stiffness and damping may be linked to the severe plastic deformation of interacting asperities under heavy axial load suggested by the hypothesis presented by Pullen and Williamson [82]. On the other hand, the interfacial damping decreased with the increase of applied torque, which agrees with the result of previous study [81].

The resistance and reactance of bolted joint under various loads (10, 30, 50, 70 N m) were obtained by using (12) and are compared in Figure 7. It can be observed that the resistance of bolted joint decreased with the increase of the applied preload (torque), which is consistent with the previous experimental results [46], [62], [83], [84]. The true contact area increased with the applied preload; in other words, the electric conductivity of the bolted joint improves with increased contact area. Thus, the resistance of bolted joint decreases as preload

$$C_n^* = \frac{C_n}{A_a^{\frac{1}{4}}\sqrt{ME^*}} = \frac{\eta\sqrt{MK_n}}{A_a^{\frac{1}{4}}\sqrt{ME^*}} = \frac{42\varphi\sqrt{\pi}(5-3D)a_c^{*(2-D)}\left\{\frac{2D}{\sqrt{\pi}(1-D)}\left(\frac{2-D}{D}\right)^{\frac{D}{2}}\psi^{\frac{(D-2)^2}{4}}A_r^{*\frac{D}{2}}\left[\psi^{\frac{-D^2+3D-2}{4}}\left(\frac{2-D}{D}\right)^{\frac{1-D}{2}}A_r^{*\left(\frac{1-D}{2}\right)} - a_c^{*\left(\frac{1-D}{2}\right)}\right]\right\}^{\frac{1}{2}}}{2^{\frac{8-D}{2}}G^{*(D-1)}(2-D)\left[\psi^{\frac{-3D^2+11D-10}{4}}\left(\frac{2-D}{D}\right)^{\frac{5-3D}{2}}A_r^{*\left(\frac{5-3D}{2}\right)} - a_c^{*\left(\frac{5-3D}{2}\right)}\right]} \tag{21}$$

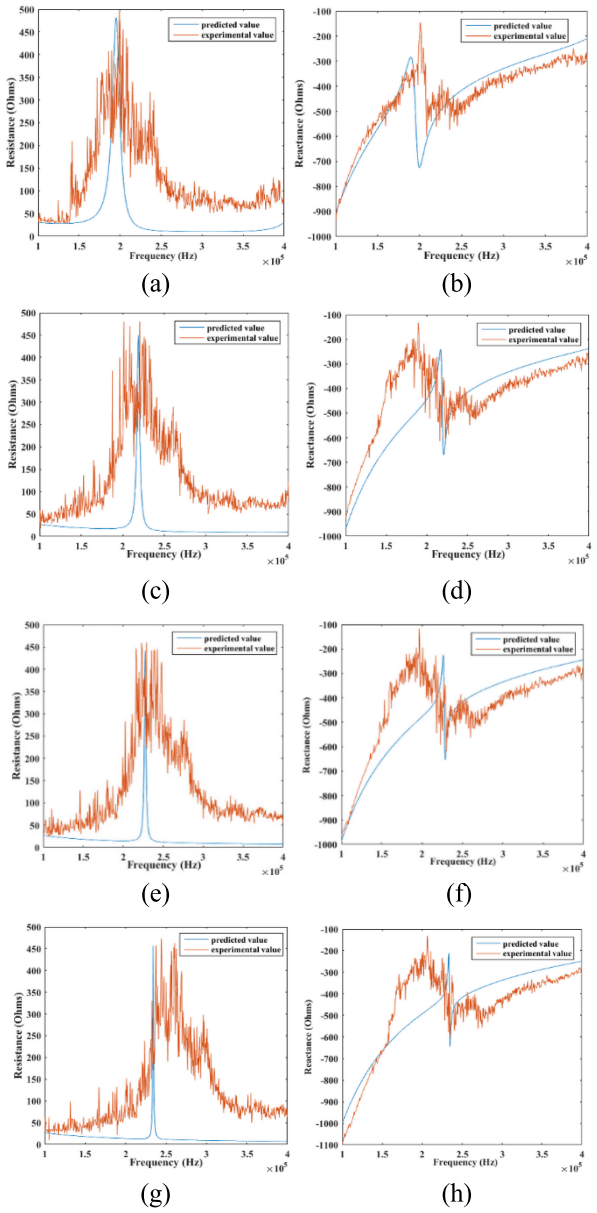

FIGURE 7. EMI of predicted and experimental values under various bolted preload. (a) Resistance under 10 N m torque. (b) Reactance under 10 N m torque. (c) Resistance under 30 N m torque. (d) Reactance under 30 N m torque. (e) Resistance under 50 N m torque. (f) Reactance under 50 N m torque. (g) Resistance under 70 N m torque. (h) Reactance under 70 N m torque.

increases. Furthermore, the peak frequency of the resistance signature also increased with the increase of the applied preload as noted in the previous studies [62], [84]–[86]. The shift in peak frequency can be attributed to the increase of the resonance frequency caused by the improved interfacial stiffness when larger preload is applied. Based on the comparative results of predicted and experimental values, the validity of the model proposed in this paper is verified. However, there exists some error due to the bonding condition of the PZT patch and the predicted error of interfacial stiffness and damping based on the fractal contact theory, which can be further improved in future research.

V. CONCLUSION

Bolted connections are widely used across engineering, however, bolted joint looseness can lead to severe accidents if not detected accurately and rapidly. In some special applications such as railway and aerospace engineering, quantitative monitoring of bolted looseness is necessary. The electromechanical impedance (EMI) method has been proven as an effective technique to monitor the bolted pre-load, however, prior work in this area was limited to experiments and were not guided by any kinds of analytical physical model. Thus, in this paper, an "effective impedance" modeling method was introduced to develop the analytical relationship between the admittance (inverse of piezoelectrical impedance) of the PZT patch and the mechanical impedance of the bolted joint. The pre-load has significant influence on the mechanical impedance of bolted joints, due to the change of stiffness and damping under different loads. Coupled with the fractal contact theory, which is a powerful tool for studying the interface, we have been able to model the stiffness and damping coefficient of bolted joint. With the model, the relationship between bolt pre-load and the piezoelectrical impedance can be obtained quantitatively. At last, the experimental results verified the validity of the proposed method. Additionally, more investigation should be conducted on the influence of the bonding layer, which can affect the force transmission between the PZT patch and the bolted joint. The bonding state in this paper is regarded as perfect; however, this assumption is too idealistic, due to often imperfect installation of the PZT patch in practical situations. Therefore, a modified EMI modeling of bolted joint considering the effect of the bonding layer should be the focus of a future study.

REFERENCES

[1] J. Xu, R. Chen, H. Chen, S. Zhang, and K. Chen, "Fast registration methodology for fastener assembly of large-scale structure," *IEEE Trans. Ind. Electron.*, vol. 64, no. 1, pp. 717–726, Jan. 2017.

[2] J. C. Olivares-Galvan, S. Magdaleno-Adame, R. Escarela-Perez, R. Ocon-Valdez, P. S. Georgilakis, and G. Loizos, "Reduction of stray losses in flange–bolt regions of large power transformer tanks," *IEEE Trans. Ind. Electron.*, vol. 61, no. 8, pp. 4455–4463, Aug. 2014.

[3] S. D. Thoppul, J. Finegan, and R. F. Gibson, "Mechanics of mechanically fastened joints in polymer–matrix composite structures—A review," *Compos. Sci. Technol.*, vol. 69, nos. 3–4, pp. 301–329, Mar. 2009.

[4] K.-Y. Jhang, H.-H. Quan, J. Ha, and N.-Y. Kim, "Estimation of clamping force in high-tension bolts through ultrasonic velocity measurement," *Ultrasonics*, vol. 44, pp. e1339–e1342, Dec. 2006.

[5] S. Chaki, G. Corneloup, I. Lillamand, and H. Walaszek, "Combination of longitudinal and transverse ultrasonic waves for *in situ* control of the tightening of bolts," *J. Pressure Vessel Technol.*, vol. 129, no. 3, pp. 383–390, Aug. 2007.

[6] X. Ding, X. Wu, and Y. Wang, "Bolt axial stress measurement based on a mode-converted ultrasound method using an electromagnetic acoustic transducer," *Ultrasonics*, vol. 54, no. 3, pp. 914–920, Mar. 2014.

[7] V. Caccese, R. Mewer, and S. S. Vel, "Detection of bolt load loss in hybrid composite/metal bolted connections," *Eng. Struct.*, vol. 26, no. 7, pp. 895–906, Jun. 2004.

[8] F. Amerini, E. Barbieri, M. Meo, and U. Polimeno, "Detecting loosening/tightening of clamped structures using nonlinear vibration techniques," *Smart Mater. Struct.*, vol. 19, no. 8, p. 085013, Aug. 2010.

[9] F. Amerini and M. Meo, "Structural health monitoring of bolted joints using linear and nonlinear acoustic/ultrasound methods," *Struct. Health Monit.*, vol. 10, no. 6, pp. 650–672, Nov. 2011.

[10] Z. Zhang, M. Liu, Z. Su, and Y. Xiao, "Quantitative evaluation of residual torque of a loose bolt based on wave energy dissipation and vibro-acoustic modulation: A comparative study," *J. Sound Vib.*, vol. 383, pp. 156–170, Nov. 2016.

[11] J. Esteban and C. A. Rogers, "Energy dissipation through joints: Theory and experiments," *Comput. Struct.*, vol. 75, no. 4, pp. 347–359, Apr. 2000.

[12] J. Yang and F.-K. Chang, "Detection of bolt loosening in C–C composite thermal protection panels: I. Diagnostic principle," *Smart Mater. Struct.*, vol. 15, no. 2, pp. 581–590, Apr. 2006.

[13] J. Yang and F.-K. Chang, "Detection of bolt loosening in C–C composite thermal protection panels: II. Experimental verification," *Smart Mater. Struct.*, vol. 15, no. 2, pp. 591–599, Apr. 2006.

[14] W. Tao, L. Shaopeng, S. Junhua, and L. Yourong, "Health monitoring of bolted joints using the time reversal method and piezoelectric transducers," *Smart Mater. Struct.*, vol. 25, no. 2, p. 025010, Feb. 2016.

[15] X. Tian, Q. Quan, L. Wang, and Q. Su, "An inchworm type piezoelectric actuator working in resonant state," *IEEE Access*, vol. 6, pp. 18975–18983, 2018.

[16] Y. Liu, W. Chen, D. Shi, X. Tian, S. Shi, and D. Xu, "Development of a four-feet driving type linear piezoelectric actuator using bolt-clamped transducers," *IEEE Access*, vol. 5, pp. 27162–27171, 2017.

[17] J. Zhao, R. Gao, S. Liu, and Y. Huang, "A new sensitivity-improving method for piezoelectric resonance mass sensors through cantilever cross-section modification," *IEEE Trans. Ind. Electron.*, vol. 61, no. 3, pp. 1612–1621, Mar. 2014.

[18] A. M. Sánchez, R. Prieto, M. Laso, and T. Riesgo, "A piezoelectric minirheometer for measuring the viscosity of polymer microsamples," *IEEE Trans. Ind. Electron.*, vol. 55, no. 1, pp. 427–436, Jan. 2008.

[19] J. Liang and W.-H. Liao, "Improved design and analysis of self-powered synchronized switch interface circuit for piezoelectric energy harvesting systems," *IEEE Trans. Ind. Electron.*, vol. 59, no. 4, pp. 1950–1960, Apr. 2012.

[20] M. H. Malakooti and H. A. Sodano, "Piezoelectric energy harvesting through shear mode operation," *Smart Mater. Struct.*, vol. 24, no. 5, p. 055005, May 2015.

[21] Z. Zhang, J. Kan, S. Wang, H. Wang, C. Yang, and S. Chen, "Performance dependence on initial free-end levitation of a magnetically levitated piezoelectric vibration energy harvester with a composite cantilever beam," *IEEE Access*, vol. 5, pp. 27563–27572, 2017.

[22] S. Siu, Q. Ji, W. Wu, G. Song, and Z. Ding, "Stress wave communication in concrete: I. Characterization of a smart aggregate based concrete channel," *Smart Mater. Struct.*, vol. 23, no. 12, p. 125030, Dec. 2014.

[23] S. Siu, Q. Ji, K. Wang, G. Song, and Z. Ding, "Stress wave communication in concrete: II. Evaluation of low voltage concrete stress wave communications utilizing spectrally efficient modulation schemes with PZT transducers," *Smart Mater. Struct.*, vol. 23, no. 12, p. 125031, Dec. 2014.

[24] B. C. Lee and W. J. Staszewski, "Modelling of Lamb waves for damage detection in metallic structures: Part I. Wave propagation," *Smart Mater. Struct.*, vol. 12, no. 5, pp. 117–162, Oct. 2003.

[25] W. J. Staszewski, S. Mahzan, and R. Traynor, "Health monitoring of aerospace composite structures—Active and passive approach," *Compos. Sci. Technol.*, vol. 69, nos. 11–12, pp. 1678–1685, Sep. 2009.

[26] C. Liang, F. P. Sun, and C. A. Rogers, "Coupled electro-mechanical analysis of adaptive material systems-determination of the actuator power consumption and system energy transfer," *J. Intell. Mater. Syst. Struct.*, vol. 5, no. 1, pp. 12–20, Jan. 1994.

[27] A. C. Rutherford, G. Park, and C. R. Farrar, "Non-linear feature identifications based on self-sensing impedance measurements for structural health assessment," *Mech. Syst. Signal Process.*, vol. 21, no. 1, pp. 322–333, Jan. 2007.

[28] T. Wandowski, P. H. Malinowski, and W. M. Ostachowicz, "Delamination detection in CFRP panels using EMI method with temperature compensation," *Compos. Struct.*, vol. 151, pp. 99–107, Sep. 2016.

[29] F. Wang, H. Zhang, C. Liang, Y. Tian, X. Zhao, and D. Zhang, "Design of high-frequency ultrasonic transducers with flexure decoupling flanges for thermosonic bonding," *IEEE Trans. Ind. Electron.*, vol. 63, no. 4, pp. 2304–2312, Apr. 2016.

[30] P. Malinowski, T. Wandowski, and W. Ostachowicz, "The use of electromechanical impedance conductance signatures for detection of weak adhesive bonds of carbon fibre–reinforced polymer," *Struct. Health Monit.*, vol. 14, no. 4, pp. 332–344, Jul. 2015.

[31] H. Zhu, H. Luo, D. Ai, and C. Wang, "Mechanical impedance-based technique for steel structural corrosion damage detection," *Measurement*, vol. 88, pp. 353–359, Jun. 2016.

[32] F. G. Baptista, J. V. Filho, and D. J. Inman, "Sizing PZT transducers in impedance-based structural health monitoring," *IEEE Sensors J.*, vol. 11, no. 6, pp. 1405–1414, Jun. 2011.

[33] V. A. D. de Almeida, F. G. Baptista, and P. R. de Aguiar, "Piezoelectric transducers assessed by the pencil lead break for impedance-based structural health monitoring," *IEEE Sensors J.*, vol. 15, no. 2, pp. 693–702, Feb. 2015.

[34] Y.-R. Wong, H. Du, and X. Pang, "Real-time electrical impedance resonance shift of piezoelectric sensor for detection of damage in honeycomb core sandwich structures," *NDT & E Int.*, vol. 76, pp. 61–65, Dec. 2015.

[35] Y. Y. Lim, S. Bhalla, and C. K. Soh, "Structural identification and damage diagnosis using self-sensing piezo-impedance transducers," *Smart Mater. Struct.*, vol. 15, no. 4, pp. 987–995, Aug. 2006.

[36] D. M. Peairs, G. Park, and D. J. Inman, "Improving accessibility of the impedance-based structural health monitoring method," *J. Intell. Mater. Syst. Struct.*, vol. 15, no. 2, pp. 129–139, Feb. 2004.

[37] Y. Y. Lim and C. K. Soh, "Fatigue life estimation of a 1D aluminum beam under mode-I loading using the electromechanical impedance technique," *Smart Mater. Struct.*, vol. 20, no. 12, p. 125001, Dec. 2011.

[38] Y. Liang, D. Li, S. M. Parvasi, and G. Song, "Load monitoring of pin-connected structures using piezoelectric impedance measurement," *Smart Mater. Struct.*, vol. 25, no. 10, p. 105011, Oct. 2016.

[39] X. Liu and Z. Jiang, "Design of a PZT patch for measuring longitudinal mode impedance in the assessment of truss structure damage," *Smart Mater. Struct.*, vol. 18, no. 12, p. 125017, Dec. 2009.

[40] C. Soh, K. K.-H. Tseng, S. Bhalla, and A. Gupta, "Performance of smart piezoceramic patches in health monitoring of a RC bridge," *Smart Mater. Struct.*, vol. 9, no. 4, pp. 533–542, Aug. 2000.

[41] D. L. Mascarenas, M. D. Todd, G. Park, and C. R. Farrar, "Development of an impedance-based wireless sensor node for structural health monitoring," *Smart Mater. Struct.*, vol. 16, no. 6, pp. 2137–2145, Dec. 2007.

[42] J. R. Wait, G. Park, and C. R. Farrar, "Integrated structural health assessment using piezoelectric active sensors," *Shock Vib.*, vol. 12, no. 6, pp. 389–405, 2005.

[43] Y.-K. An and H. Sohn, "Integrated impedance and guided wave based damage detection," *Mech. Syst. Signal Process.*, vol. 28, pp. 50–62, Apr. 2012.

[44] S. Park, S. Ahmad, C.-B. Yun, and Y. Roh, "Multiple crack detection of concrete structures using impedance-based structural health monitoring techniques," *Experim. Mech.*, vol. 46, no. 5, pp. 609–618, 2006.

[45] G. Park, H. H. Cudney, and D. J. Inman, "Impedance-based health monitoring of civil structural components," *J. Infrastruct. Syst.*, vol. 6, no. 4, pp. 153–160, Dec. 2000.

[46] G. Park, H. H. Cudney, and D. J. Inman, "Feasibility of using impedance-based damage assessment for pipeline structures," *Earthquake Eng. Struct. Dyn.*, vol. 30, no. 10, pp. 1463–1474, Oct. 2001.

[47] C. Liang, F. P. Sun, and C. A. Rogers, "An impedance method for dynamic analysis of active material systems," *J. Vib. Acoust.*, vol. 116, no. 1, pp. 120–128, Jan. 1994.

[48] C. Liang, F. Su, and C. A. Rogers, "Electro-mechanical impedance modeling of active material systems," *Smart Mater. Struct.*, vol. 5, no. 2, pp. 171–186, Apr. 1996.

[49] V. Giurgiutiu and A. N. Zagrai, "Embedded self-sensing piezoelectric active sensors for on-line structural identification," *J. Vib. Acoust.*, vol. 124, no. 1, pp. 116–125, Jan. 2002.

[50] S.-W. Zhou, C. Liang, and C. A. Rogers, "An impedance-based system modeling approach for induced strain actuator-driven structures," *J. Vib. Acoust.*, vol. 118, no. 3, pp. 323–331, Jul. 1996.

[51] Y. Yang, J. Xu, and C. K. Soh, "Generic impedance-based model for structure-piezoceramic interacting system," *J. Aerosp. Eng.*, vol. 18, no. 2, pp. 93–101, Apr. 2005.

[52] S. Bhalla and C. K. Soh, "Structural health monitoring by piezo–impedance transducers. I: Modeling," *J. Aerosp. Eng.*, vol. 17, no. 4, pp. 154–165, Oct. 2004.

[53] S. Bhalla and C. K. Soh, "Structural health monitoring by piezo–impedance transducers. II: Applications," *J. Aerosp. Eng.*, vol. 17, no. 4, pp. 166–175, Oct. 2004.

[54] V. G. M. Annamdas and C. K. Soh, "Three-dimensional electromechanical impedance model. I: Formulation of directional sum impedance," *J. Aerosp. Eng.*, vol. 20, no. 1, pp. 53–62, Jan. 2007.

[55] V. G. M. Annamdas and C. K. Soh, "Three-dimensional electromechanical impedance model for multiple piezoceramic transducers—Structure interaction," *J. Aerosp. Eng.*, vol. 21, no. 1, pp. 35–44, Jan. 2007.

[56] V. G. M. Annamdas and C. K. Soh, "Embedded piezoelectric ceramic transducers in sandwiched beams," *Smart Mater. Struct.*, vol. 15, no. 2, pp. 538–549, Apr. 2006.
[57] W. Yan, C. W. Lim, J. B. Cai, and W. Q. Chen, "An electromechanical impedance approach for quantitative damage detection in Timoshenko beams with piezoelectric patches," *Smart Mater. Struct.*, vol. 16, no. 4, pp. 1390–1400, Aug. 2007.
[58] A. N. Zagrai and V. Giurgiutiu, "Electro-mechanical impedance method for crack detection in thin plates," *J. Intell. Mater. Syst. Struct.*, vol. 12, no. 10, pp. 709–718, Oct. 2001.
[59] S.-W. Zhou, C. Liang, and C. A. Rogers, "Modeling of distributed piezoelectric actuators integrated with thin cylindrical shells," *J. Acoust. Soc. Amer.*, vol. 96, no. 3, pp. 1605–1612, Sep. 1994.
[60] Y. Yang and Y. Hu, "Electromechanical impedance modeling of PZT transducers for health monitoring of cylindrical shell structures," *Smart Mater. Struct.*, vol. 17, no. 1, p. 015005, Feb. 2008.
[61] S. Ritdumrongkul, M. Abe, Y. Fujino, and T. Miyashita, "Quantitative health monitoring of bolted joints using a piezoceramic actuator–sensor," *Smart Mater. Struct.*, vol. 13, no. 1, pp. 20–29, Feb. 2004.
[62] S. Ritdumrongkul and Y. Fujino, "Identification of the location and level of damage in multiple-bolted-joint structures by PZT actuator-sensors," *J. Struct. Eng.*, vol. 132, no. 2, pp. 304–311, Feb. 2006.
[63] A. Majumdar and B. Bhushan, "Fractal model of elastic-plastic contact between rough surfaces," *J. Tribol.*, vol. 113, no. 1, pp. 1–11, Jan. 1991.
[64] J. A. Greenwood and J. B. P. Williamson, "Contact of nominally flat surfaces," *Proc. Roy. Soc. Lond. A, Math. Phys. Sci.*, vol. 295, no. 1442, pp. 300–319, 1966.
[65] L. Huo, F. Wang, H. Li, and G. Song, "A fractal contact theory based model for bolted connection looseness monitoring using piezoceramic transducers," *Smart Mater. Struct.*, vol. 26, no. 10, p. 104010, Oct. 2017.
[66] F. Wang, L. Huo, and G. Song, "A piezoelectric active sensing method for quantitative monitoring of bolt loosening using energy dissipation caused by tangential damping based on the fractal contact theory," *Smart Mater. Struct.*, vol. 27, no. 1, p. 015023, Jan. 2018.
[67] S. Wang and K. Komvopoulos, "A fractal theory of the interfacial temperature distribution in the slow sliding regime: Part I—Elastic contact and heat transfer analysis," *J. Tribol.*, vol. 116, no. 4, pp. 812–823, Oct. 1994.
[68] S. Wang and K. Komvopoulos, "A fractal theory of the interfacial temperature distribution in the slow sliding regime: Part II—Multiple domains, elastoplastic contacts and applications," *J. Tribol.*, vol. 116, no. 4, pp. 824–832, Oct. 1994.
[69] S. Jiang, Y. Zheng, and H. Zhu, "A contact stiffness model of machined plane joint based on fractal theory," *J. Tribol.*, vol. 132, no. 1, p. 011401, Nov. 2009.
[70] Y. Zhao, D. David, and L. Chang, "An asperity microcontact model incorporating the transition from elastic deformation to fully plastic flow," *J. Tribol.*, vol. 122, no. 1, pp. 86–93, May 1999.
[71] J. Sirohi and I. Chopra, "Fundamental understanding of piezoelectric strain sensors," *J. Intell. Mater. Syst. Struct.*, vol. 11, no. 4, pp. 246–257, Apr. 2000.
[72] S. Zhou, C. Liang, and C. A. Rogers, "Integration and design of piezoceramic elements in intelligent structures," *J. Intell. Mater. Syst. Struct.*, vol. 8, no. 4, pp. 363–373, Apr. 1997.
[73] E. L. Hixon, "Mechanical impedance," in *Shock Vibration Handbook*, 3rd ed. New York, NY, USA: McGraw-Hill, 1988, pp. 10.1-10.46.
[74] K. L. Johnson, *Contact Mechanics*. Cambridge, U.K.: Cambridge Univ. Press, 1985.
[75] W. Yan and K. Komvopoulos, "Contact analysis of elastic-plastic fractal surfaces," *J. Appl. Phys.*, vol. 84, no. 7, pp. 3617–3624, Oct. 1998.
[76] D. Tabor, *The Hardness of Metals*. Oxford, U.K.: Clarendon, 1951.
[77] A. Majumdar and C. L. Tien, "Fractal characterization and simulation of rough surfaces," *Wear*, vol. 136, no. 2, pp. 313–327, Mar. 1990.
[78] H. Zhu, S. Ge, X. Huang, D. Zhang, and J. Liu, "Experimental study on the characterization of worn surface topography with characteristic roughness parameter," *Wear*, vol. 255, nos. 1–6, pp. 309–314, Aug./Sep. 2003.
[79] G. Sauerbrey, "Verwendung von Schwingquarzen zur Wägung Dünner Schichten und zur Mikrowägung," *Zeitschrift Phys.*, vol. 155, no. 2, pp. 206–222, 1959.
[80] C. R. Farrar, G. Park, H. Sohn, and D. J. Inman, "Overview of piezoelectric impedance-based health monitoring and path forward," *Shock Vib. Dig.*, vol. 35, no. 6, pp. 451–463, Nov. 2003.
[81] W. P. Fu, Y. M. Huang, X. L. Zhang, and Q. Guo, "Experimental investigation of dynamic normal characteristics of machined joint surfaces," *J. Vib. Acoust.*, vol. 122, no. 4, pp. 393–398, Oct. 2000.
[82] J. Pullen and J. B. P. Williamson, "On the plastic contact of rough surfaces," *Proc. Roy. Soc. A, Math. Phys. Eng. Sci.*, vol. 327, no. 1569, pp. 159–173, Mar. 1972.
[83] I. Pavelko, V. Pavelko, S. Kuznestsov, and I. Ozolinsh, "Bolt-joint structural health monitoring by the method of electromechanical impedance," *Aircr. Eng. Aerosp. Technol.*, vol. 86, no. 3, pp. 207–214, 2014.
[84] C. He, S. Yang, Z. Liu, and B. Wu, "Damage localization and quantification of truss structure based on electromechanical impedance technique and neural network," *Shock Vib.*, vol. 2014, Jun. 2014, Art. no. 727404.
[85] S. Park, H.-H. Shin, and C.-B. Yun, "Wireless impedance sensor nodes for functions of structural damage identification and sensor self-diagnosis," *Smart Mater. Struct.*, vol. 18, no. 5, p. 055001, May 2009.
[86] D. Doyle, A. Zagrai, B. Arritt, and H. Cakan, "Damage detection in bolted space structures," *J. Intell. Mater. Syst. Struct.*, vol. 21, no. 3, pp. 251–264, Feb. 2010.

FURUI WANG received the B.S. and M.S. degrees from the Department of Mechanical Engineering, Dalian University of Technology, in 2014 and 2017, respectively. He is currently pursuing the Ph.D. degree in mechanical engineering with the University of Houston. He has published over 10 peer-reviewed journal articles. His research interests include structural health monitoring, smart materials and structures, and analytical/numerical modeling.

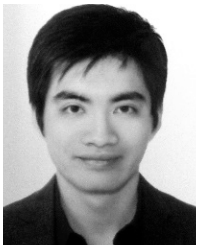

SIU CHUN MICHAEL HO received the B.S. degree from the Department of Biomedical Engineering and the M.S. and Ph.D. degrees from the Department of Mechanical Engineering, University of Houston, in 2008, 2010, and 2012, respectively. He has lectured laboratory courses at the University of Houston. He is currently a Research Associate with the Department of Mechanical Engineering, University of Houston. He published over 33 peer-reviewed journal articles, including a *Smart Materials and Structures* Journal Highlight of 2015, and 11 conference articles. His research interests include the application of fiber optic sensors for structural health monitoring, vibration analysis, biomedical devices, and intelligent structures.

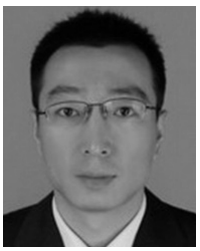

LINSHENG HUO received the B.S. and M.S. degrees from the Department of Civil Engineering, Shenyang Jianzhu University, China, in 2001 and 1998, respectively, and the Ph.D. degree from the School of Civil Engineering, Dalian University of Technology, China, in 2005. He is currently an Associate Professor with the School of Civil Engineering, Dalian University of Technology. He has expertise in structural vibration control, smart materials and structures, piezoceramics, and structural engineering.

GANGBING SONG received the B.S. degree from Zhejiang University, China, in 1989, and the M.S. and Ph.D. degrees from the Department of Mechanical Engineering, Columbia University, New York, in 1995 and 1991, respectively. He is currently the Founding Director of the Smart Materials and Structures Laboratory and a Professor of mechanical engineering, civil and environmental engineering, and electrical and computer engineering with the University of Houston. He has developed two new courses in smart materials and published over 400 papers, including 196 peer reviewed journal articles. He has expertise in smart materials and structures, structural vibration control, piezoceramics, ultrasonic transducers, structural health monitoring, and damage detection. He was a recipient of the NSF CAREER Award in 2001.